

# Food & Function

Linking the chemistry and physics of food with health and nutrition

Accepted Manuscript

This article can be cited before page numbers have been issued, to do this please use: F. Song, H. Ding, Y. Chen, X. Ge, R. Guo, F. Wu, Y. Guo, R. Gan and Z. Chen, *Food Funct.*, 2026, DOI: 10.1039/D6FO00232C.



This is an Accepted Manuscript, which has been through the Royal Society of Chemistry peer review process and has been accepted for publication.

Accepted Manuscripts are published online shortly after acceptance, before technical editing, formatting and proof reading. Using this free service, authors can make their results available to the community, in citable form, before we publish the edited article. We will replace this Accepted Manuscript with the edited and formatted Advance Article as soon as it is available.

You can find more information about Accepted Manuscripts in the [Information for Authors](#).

Please note that technical editing may introduce minor changes to the text and/or graphics, which may alter content. The journal's standard [Terms & Conditions](#) and the [Ethical guidelines](#) still apply. In no event shall the Royal Society of Chemistry be held responsible for any errors or omissions in this Accepted Manuscript or any consequences arising from the use of any information it contains.

1           **Dihydromyricetin Attenuates Platelet Hyperactivity in**  
2           **HFD/STZ-Induced Diabetic Mice by Inhibiting Intraplatelet ROS**  
3           **Generation**

4  
5           Fenglin Song<sup>a,b,#</sup>, Huafang Ding<sup>a,#</sup>, Yun Chen<sup>a</sup>, Xiangzhen Ge<sup>a</sup>, Ruixue Guo<sup>a</sup>, Fangfang  
6           Wu<sup>a</sup>, Yu Guo<sup>d</sup>, Ren-You Gan<sup>b,c,\*</sup>, Zhen-Yu Chen<sup>a,e\*</sup>

7  
8           <sup>a</sup> School of Food Science, Guangdong Pharmaceutical University, Zhongshan,  
9           Guangdong Province, 528458, China;

10          <sup>b</sup> Department of Food Science and Nutrition, The Hong Kong Polytechnic University,  
11          Hung Hom, Kowloon, Hong Kong, 999077, China;

12          <sup>c</sup> Research Institute for Future Food, The Hong Kong Polytechnic University, Hung Hom,  
13          Kowloon, Hong Kong, 999077, China.

14          <sup>d</sup> Department of blood transfusion, The First Affiliated Hospital of Guangdong  
15          Pharmaceutical University, Guangzhou, Guangdong Province, 510062, China;

16          <sup>e</sup> School of Life Sciences, The Chinese University of Hong Kong, Shatin, NT, Hong Kong,  
17          China

18  
19          # These authors contributed equally.

20          \***Correspondence:**

21          Ren-You Gan

22          Department of Food Science and Nutrition, The Hong Kong Polytechnic University,  
23          Hung Hom, Kowloon, Hong Kong SAR, 999077, China.

24          E-mail: [renyou.gan@polyu.edu.hk](mailto:renyou.gan@polyu.edu.hk)

25          Zhen-Yu Chen, Professor

26          School of Food Science, Guangdong Pharmaceutical University, Zhongshan,  
27          Guangdong Province, 528458, China.

28          E-mail: [zhenyuchen@cuhk.edu.hk](mailto:zhenyuchen@cuhk.edu.hk)

29



30 **Abstract**

31 The interaction between polyphenols and platelets is an emerging area in  
32 understanding how diet affects heart disease. Platelet hyperactivity is one of critical  
33 drivers of cardiovascular complications in Type 2 diabetes mellitus (T2DM). As one of  
34 the abundant polyphenols in nature, dihydromyricetin (DHM) has been shown to  
35 inhibit platelet activation and aggregation *in vitro*. This study aimed to investigate the  
36 *in vivo* effects and potential mechanisms of dietary DHM supplementation on platelet  
37 hyperactivity in diabetic mice. T2DM mouse model was established by feeding a high-  
38 fat diet (HFD) combined with streptozotocin (STZ) injection, followed by dietary  
39 supplementation with DHM (500 or 1000 mg/kg in diets) for eight weeks. Flow  
40 cytometric analysis revealed that DHM significantly reduced platelet surface  
41 expression of CD62P, CD63, and CD40 ligands, decreased integrin  $\alpha\text{IIb}\beta\text{3}$  activation,  
42 and suppressed intraplatelet reactive oxygen species (ROS) production. The  
43 exaggerated platelet aggregation and ATP secretion induced by thrombin and collagen  
44 were also markedly attenuated. Additionally, DHM reduced plasma levels of *in vivo*  
45 platelet activation markers, soluble P-selectin, platelet factor 4, thromboxane B2, and  
46 the oxidative stress marker 8-iso-prostaglandin F2 $\alpha$ . DHM administration also delayed  
47 collagen/epinephrine-induced pulmonary embolism formation without prolonging tail  
48 bleeding time in T2DM mice. Molecular docking suggested binding interactions  
49 between DHM with NADPH oxidase-2, aldose reductase, and platelet receptor PAR-1,  
50 GPVI, as well as COX-1. Collectively, dietary DHM attenuated platelet hyperactivity and  
51 thrombus formation in T2DM mice, primarily through suppression of intraplatelet ROS  
52 formation. These findings highlight DHM as a promising natural candidate for  
53 preventing diabetic cardiovascular complications.

54 **Keywords:** *Dihydromyricetin; Platelet; Type 2 diabetes mellitus; Reactive oxygen*  
55 *species.*

56



## 57 1. Introduction

58 Dietary flavonoids may be associated with reduced risk of cardiovascular diseases  
59 by down-regulation of platelet activity. Platelets play a pivotal role in both  
60 physiological hemostasis and pathological thrombosis formation.<sup>1</sup> Enhanced platelet  
61 reactivity as the consequence of some pathological conditions, such as hyperlipidemia,  
62 hyperglycemia, obesity, hypertension, and dysbiosis, can lead to pathological  
63 thrombus formation, which ultimately contributes to blood vessel stenosis, ischemia,  
64 and myocardial infarction.<sup>2, 3</sup> Type 2 Diabetes mellitus (T2DM) is well established as a  
65 critical risk factor for cardiovascular diseases (CVDs).<sup>4</sup> Individuals with T2DM have a 2-  
66 4 folds risk of CVDs compared to non-diabetic individuals, and up to 80% of these  
67 diabetic subjects will die due to CVDs.<sup>5</sup> Increased responsiveness of platelets  
68 (hyperactivity) in T2DM has been recognized as a critical driver for cardiovascular  
69 disorders.<sup>6</sup> As a previous study reported, platelets from patients with T2DM exhibited  
70 intensified adhesion, activation, and aggregation, along with increased fibrinogen  
71 binding and surface expression of CD62P, increased production of TXA2 and  
72 superoxide anion.<sup>7</sup> Additionally, plasma derived from T2DM patients contains  
73 elevated concentrations of platelet activation markers, such as soluble (sCD40L), PF-  
74 4, and sP-selectin.<sup>8</sup>

75 Platelet hyperactivity is not only related to hyperglycemia, but also associated  
76 with various metabolic comorbidities commonly found in Diabetes mellitus, including  
77 insulin resistance, dyslipidemia, obesity, systemic inflammation and oxidative stress.<sup>9</sup>  
78 The oxidative damage of platelets and activation of pro-oxidant enzymes, such as  
79 NADPH oxidase (NOX) and aldose reductase (AR), appear to be central to platelet  
80 hyperactivity in diabetes.<sup>10</sup> However, current anti-platelet drugs including aspirin and  
81 clopidogrel, exhibit reduced efficacy in diabetic patients, which is, at least in part,  
82 attributed to diabetes-associated oxidative stress.<sup>11, 12</sup> Furthermore, antiplatelet drugs  
83 can cause some serious side effects, including bleeding episodes, gastrointestinal  
84 toxicity, neutropenia, and thrombocytopenia. Therefore, the development of  
85 alternative or natural anti-platelet bioactive compounds is urgently needed to reduce  
86 CVD risk in T2DM patients.



87 Many dietary components such as anthocyanins, quercetin, resveratrol, curcumin  
88 sulforaphane and gallic acid have been reported to inhibit platelet functions and  
89 thrombus formation through distinct mechanisms.<sup>13-17</sup> Meanwhile, these natural  
90 compounds were found to be safe and did not increase bleeding risks. Thus, dietary  
91 intake of bioactive compounds with a platelet inhibitory activity should be effective to  
92 fight against the continued platelet hyperactivity in response to inappropriate  
93 nutritional and lifestyle factors including hyperglycemia and hyperlipidemia.<sup>3</sup>  
94 Dihydromyricetin (DHM) is widely abundant in plants such as Chinese vine tea, grapes,  
95 mulberries, and ginkgo biloba.<sup>18</sup> DHM has demonstrated numerous biological  
96 activities, such as antioxidant, anti-inflammation and cardiovascular protection.<sup>19</sup> A  
97 previous *in vitro* study also demonstrated that DHM effectively inhibited thrombin-  
98 induced platelet activation, aggregation, and spreading.<sup>20</sup> However, the effects of  
99 DHM on platelet function *in vivo* have not yet been investigated. Specifically, it  
100 remains unclear whether DHM can effectively mitigate the persistent platelet  
101 hyperactivity induced by chronic hyperglycemia and systemic metabolic dysregulation.

102 The present study aimed to investigate the *in vivo* effects and potential  
103 mechanisms of DHM on high platelet reactivity in diabetic mice. Firstly, a diabetic  
104 mouse model was induced by feeding a high-fat diet (HFD) combining with  
105 intraperitoneal injection of streptozotocin (STZ). Secondly, the effects of DHM  
106 supplementation on platelet hyperactivity in diabetic mice was examined by  
107 measuring platelet activation, aggregation, granule secretion, and ROS production, as  
108 well as the *in vivo* platelet activation markers in plasma. Lastly, collagen/epinephrine-  
109 induced pulmonary embolism was induced in mice, and the alleviating effect of DHM  
110 on thrombus formation in T2DM mice was investigated.

## 111 2. Materials and methods

### 112 2.1 Materials

113 DHM (purity $\geq$ 99%) was purchased from Zelang Medical Technology Co., Ltd  
114 (Nanjing, China). Streptozotocin (STZ) was purchased from Shanghai Aladdin Biological



115 Technology Co., Ltd (Shanghai, China). Platelet agonist thrombin was purchased from  
116 Sigma-Aldrich (St Louis, MO, USA). Collagen and luciferase-luciferin reagent were from  
117 Chrono-log (Havertown, PA, USA). APC-conjugated anti-mouse CD63 antibody, FITC-  
118 conjugated anti-mouse CD62P antibody and PE-conjugated anti-mouse CD40L  
119 antibody were obtained from BD Biosciences (San Diego, CA). PE-conjugated JON/A  
120 was purchased from Emfret Analytics (Eibelstadt, Germany). 5-(and 6)-chloromethyl-  
121 2',7'-dichlorodihydrofluorescein diacetate (CM-H2DCFDA) was obtained from Thermo  
122 Fisher Scientific (Waltham, MA, USA). All other chemicals were of reagent grade.

## 123 2.2 Animals and treatment

124 Six-week-old male C57BL/6 mice were purchased from Zhuhai BesTest Bio-  
125 Tech Co. Ltd (Zhuhai, Guangdong, China). All animal procedures were approved by  
126 the Animal Care and Protection Committee of Guangdong Pharmaceutical University  
127 (Permit No. 2023212) and were performed in accordance with the National Institutes  
128 of Health Guide for the Care and Use of Laboratory Animals. In general, Type 1  
129 Diabetes can be induced by a single and high dose of STZ, which causes significant  
130 beta-cell loss, leading to absolute insulin deficiency, whereas Type 2 Diabetes can be  
131 induced by low-doses of STZ, often combined with a high-fat diet, which creates  
132 insulin resistance and modest hyperglycemia. The overall experimental design and  
133 procedures of the study are presented in Figure S1. Experimental Type 2 diabetic mice  
134 were induced as previously described.<sup>21</sup> Mice were fed a high-fat diet (HFD) (60%  
135 calorie from fat, TP23400, Trophic Animal Feed High-Tech Co. Ltd., Nantong, China),  
136 and the detailed diet composition was shown in Table S1. After four weeks, mice were  
137 given an intraperitoneal injection of STZ dissolved in the citrate buffer (pH 4.5) at a  
138 daily dose of 40 mg/kg b.w. for five consecutive days in the fifth week. Meanwhile,  
139 normal control mice (NG) were fed a common diet throughout the entire  
140 experimental period and received an intraperitoneal injection with the citrate buffer.  
141 Fasting blood glucose (FBG) levels were examined in a week after STZ injection, and  
142 mice with FBG levels higher than 11.1 mmol/L were considered diabetic. After  
143 successful model establishment, the diabetic mice were further divided into three  
144 groups, including the high glycemia group (HG) that mice were fed the HFD, the HG-L



145 group that mice were fed the HFD with a low dose of DHM (500 mg/kg diet), and the  
146 HG-H group that mice were fed the HFD with a high dose of DHM (1000 mg/kg diet).  
147 Based on average food consumption, the dietary doses of DHM correspond to  
148 approximately 60 and 120 mg/kg/day in mice. These doses were selected based on  
149 previous *in vivo* studies demonstrating their metabolic efficacy and safety.<sup>22, 23</sup> After  
150 eight weeks, mice were anaesthetized with 3% isoflurane via inhalation, and blood  
151 samples were collected for the preparation of gel-filtered platelets and subsequent  
152 assays.

### 153 2.3 Tail vein bleeding assay

154 As a measurement of the hemostatic function, tail bleeding time was determined  
155 at the end of the treatment period. As previously described,<sup>24</sup> mice were anesthetized  
156 and 3 mm segment of the distal tail tip was amputated with a sharp scalpel. The tail  
157 was immediately immersed in normal saline that has been pre-warmed to 37 °C. The  
158 time from incision to cessation of bleeding was recorded as the bleeding time. If  
159 bleeding did not stop spontaneously, it was stopped by cauterization at 600 seconds.

### 160 2.4 Hematological study and plasma lipid determinations

161 After the determination of tail bleeding time, blood samples were collected and  
162 the anticoagulated whole blood was analyzed using an automatic multi-parameter  
163 blood cell counter SysmexXP-300 (Sysmex Corporation, Kobe, Japan). Hematological  
164 parameters, including red blood cells (RBCs) count, hematocrit (HCT), hemoglobin (Hb)  
165 concentration, white blood cells (WBCs), platelets (PLT), mean corpuscular volume  
166 (MCV), and mean platelet volume (MPV), were analyzed using standard methods.  
167 Plasma levels of total cholesterol (TC), total triglyceride (TG), low-density lipoprotein  
168 cholesterol (LDL-C) and high-density lipoprotein cholesterol (HDL-C) were measured  
169 spectrophotometrically following the kit protocol.

### 170 2.5 Gel-filtered platelet preparation

171 The whole blood of mice was collected into a tube containing acid-citrate-



172 dextrose (ACD, 1/9, v/v), and was incubated at 37 °C for 10 min. Platelet-rich plasma  
173 (PRP) was obtained from blood samples by centrifugation at 300 × g for 7 min at room  
174 temperature. Gel-filtered platelets were isolated from PRP using a Sepharose 2B  
175 column in PIPES buffer (5 mmol/L PIPES, 1.37 mmol/L NaCl, 4 mmol/L KCl, 0.1% (w/v)  
176 glucose, pH 7.0) according to our previously described method.<sup>25</sup> Due to the limited  
177 blood volume obtained from individual mice and the requirement for concomitant  
178 hematological analysis and plasma preparation, gel-filtered platelets were randomly  
179 pooled from two mice within the same group to obtain sufficient gel-filtered platelets.  
180 Each pooled sample was treated as a single independent biological replicate.

181

## 182 2. 6 Platelet aggregation and ATP release measurement

183 Platelet aggregation and ATP release were simultaneously measured in Chrono-  
184 log aggregometer (Chrono-Log, Havertown, PA, USA). Briefly, the gel-filtered platelets  
185 were pooled from two mice of each group and adjusted to  $3 \times 10^8$  cells/mL. Luciferin-  
186 luciferase reagent was added directly to platelet suspensions followed by the  
187 stimulation with 0.1 U/mL thrombin or 1 µg/mL collagen in the presence of 1 mmol/L  
188  $\text{Ca}^{2+}$ . Then real-time platelet aggregation and ATP secretion was recorded over a  
189 period of 6 min.

## 190 2.7 Flow cytometry

191 Gel-filtered platelets were adjusted to  $1 \times 10^6$  cells /mL and were preincubated  
192 with FITC-conjugated anti-mouse CD62P, PE-conjugated anti-mouse CD40L, PE-  
193 conjugated JON/A, or FITC-conjugated anti-mouse CD63 for 15 min at room  
194 temperature in the dark. The labeled platelets were then activated with thrombin or  
195 collagen for 5 min and fixed by adding 1% paraformaldehyde. All samples were  
196 analyzed by flow cytometry using the CytoFLEX flow cytometer (Beckman Coulter Inc.,  
197 CA, USA). Ten thousand platelet events were acquired per sample and the mean  
198 fluorescence intensity of positive platelets was analyzed.



199 For reactive oxygen species (ROS) determination, gel-filtered platelets were  
200 incubated with 10  $\mu$ M CM-H<sub>2</sub>DCFDA, a ROS-sensitive fluorescent probe, for 30 min at  
201 37 °C in the dark. The excessive dye was removed and platelets were resuspended in  
202 the PIEPS buffer. Then, 0.5U/mL thrombin or 2  $\mu$ g/mL collagen were added to  
203 stimulate platelets for 30 min, and the intracellular ROS generation was immediately  
204 detected by flow cytometry. These agonists concentrations were specifically  
205 optimized to ensure a detectable oxidative burst. In contrast, sub-maximal  
206 concentrations were used in platelet aggregation and activation assays to prevent  
207 saturated responses and allow accurate assessment of the inhibitory potential of DHM.

## 208 **2.8 Determination of sP-selectin, PF4, TXB<sub>2</sub>, and 8-iso-PGF<sub>2</sub> $\alpha$**

209 Commercial enzyme-linked immunosorbent assay kits were used to measure  
210 plasma levels of sP-selectin (R&D Systems, Minneapolis, MN, USA) and PF4  
211 (eBioscience, San Diego, CA, USA). The contents of TXB<sub>2</sub> and 8-iso-PGF<sub>2</sub> $\alpha$  in plasma  
212 were also determined by TXB<sub>2</sub> quantikine and 8-iso-PGF<sub>2</sub> $\alpha$  quantikine ELISA kits from  
213 ENZO Life Science (New York, USA), respectively, in accordance with the  
214 manufacturer's protocols.

## 215 **2.9 Molecular docking analysis**

216 To investigate the interactions between DHM and key receptors and catalytic  
217 enzyme involved in platelet ROS production and platelet hyperactivity, molecular  
218 docking analysis was performed as previously describe.<sup>26</sup> Briefly, the 3-dimensional  
219 chemical structure of DHM was obtained from PubChem database, while the crystal  
220 structure of PAR-1(PDB:3VW7), GPVI (PDB:2GI7), COX-1 (PDB:6Y3C), NOX-2  
221 (PDB :8GZ3) and aldose reductase (AR, PDB:1US0) were downloaded from the RCSB  
222 Protein Data Bank (<http://www.rcsb.org/>). Protein structures were preprocessed by  
223 removing all crystallographic water molecules in PyMOL 3.0 and the polar hydrogen  
224 atoms were added using AutoDockTools 1.5.7. Then, molecular docking simulations  
225 were performed using AutoDock Vina (version 1.1.2) to calculate the binding affinities  
226 between DHM and target proteins. The grid box for each target protein was defined



227 to encompass the active binding site based on the location of co-crystallized ligands  
228 or reported key residues. The grid box center coordinates and dimensions for each  
229 protein are provided in Table S3. The exhaustiveness parameter was set to 30 to  
230 ensure sufficient conformational sampling. For each docking simulation, the top 15  
231 binding poses were generated, and the best-ranked pose based on binding affinity was  
232 selected for further analysis. Additionally, the 3D interaction diagrams were generated  
233 by PyMOL 3.0 and post-docking analyses were performed using LigPlot+ to identify  
234 and quantify the intermolecular bonding interactions between DHM and the amino  
235 acid residues within the active pockets of target proteins.

## 236 **2.10 Acute pulmonary thromboembolism in mice**

237 To investigate the effect of DHM on thrombosis *in vivo*, the collagen- and  
238 epinephrine-induced acute pulmonary thromboembolism experiment was performed  
239 as previously described.<sup>27</sup> Briefly, mice were challenged with a mixture of collagen  
240 (430 µg/kg) and epinephrine (20 µg/kg) by smooth injection into one of the tail veins.  
241 The survival time of mice was determined by monitoring chest palpations, and death  
242 was determined when spontaneous respiratory chest expansions ceased for 1 min.  
243 The lungs of mice were then removed and immediately fixed in 4% paraformaldehyde  
244 for hematoxylin-eosin (HE) staining and observed under a light microscope.

## 245 **2.11 Statistical analysis**

246 Data are expressed as mean  $\pm$  standard deviation (SD). The specific sample size  
247 (n) for each individual experiment is indicated in the corresponding figure legends.  
248 Differences between groups were analyzed by one-way ANOVA followed by Student-  
249 Newman-Keuls multiple comparison test. For survival analyses as represented by  
250 Kaplan-Meier curves, a log-rank (Mantel-Cox) test was performed. All data were  
251 analyzed with SPSS software. *p*-value <0.05 was defined statistical significance.

## 252 **3. Results**

### 253 **3.1 Effects of DHM on the physiological changes in diabetic mice**



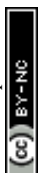
254 The initial body weight of mice for all groups was similar (Table 1). At the end of  
255 the study, diabetic mice in the HG group had a significant increase in body weight ( $p <$   
256 0.05) and liver index ( $p < 0.001$ ) compared with the NG group. As shown in Table 2,  
257 significant increases of the fasting blood glucose while a dramatical decrease of HDL-  
258 C levels were also found in the HG group. After DHM (1000 mg/kg) treatment for 8  
259 weeks, the fasting blood glucose significantly decreased in mice of the HG-H group ( $p$   
260  $< 0.01$ ). The TG/HDL-C ratio, a highly sensitive surrogate marker for insulin  
261 resistance,<sup>28</sup> was significantly elevated in HG group compared to NG group ( $P < 0.05$ ),  
262 confirming the development of insulin resistance in our model. Notably, DHM  
263 supplementation significantly attenuated this ratio in HG-H group compared to the HG  
264 group ( $P < 0.05$ ), suggesting an improvement in insulin sensitivity. No statistically  
265 significant differences were observed in hematological parameters among the four  
266 groups (Table S1).

### 267 3.2 DHM decreased platelet aggregation in diabetic mice

268 To evaluate whether DHM affects platelet hyperactivity in diabetic mice, platelet  
269 aggregation was measured after stimulation with either thrombin or collagen. As  
270 shown in Figure 1A, platelet aggregation rate induced by thrombin was  $78.30 \pm 5.23\%$   
271 in the HG group mice, which was significantly higher than that in the NG control mice  
272 ( $57.11 \pm 9.88\%$ ,  $p < 0.001$ ). The addition of 1000 mg/kg DHM normalized thrombin-  
273 induced platelet hyperaggregability to the level of the NG group. Consistently, platelet  
274 aggregation induced by collagen was also significantly greater in gel-filtered platelets  
275 separated from the HG group compared with the NG group ( $65.64 \pm 9.44\%$  and  $49.73$   
276  $\pm 8.40\%$ , respectively). Similarly, the treatment of DHM in HG-L and HG-H groups  
277 remarkably inhibited platelet aggregation induced by collagen (Figure 1B).

### 278 3.3 DHM reduced platelet ATP secretion in diabetic mice

279 To further determine the effects of DHM supplementation on platelet dense  
280 granule secretion in diabetic mice, ATP secretion from gel-filtered platelets was  
281 detected. When compared to the NG group, a significant increase in ATP secretion



282 induced by thrombin was observed in the HG group ( $p < 0.001$ , Figure 2A). DHM  
283 treatment dramatically decreased platelet ATP secretion in both HG-L and HG-H  
284 groups ( $1.12 \pm 0.13$  and  $1.04 \pm 0.28$  nmol/mL, respectively). Similar trends among  
285 these groups were also observed in collagen-induced platelet ATP secretion (Figure  
286 2B). DHM treatment at the dose of 1000 mg/kg significantly normalized collagen-  
287 induced platelet ATP secretion to levels of the NG group.

### 288 **3.4 DHM attenuated platelet activation in diabetic mice**

289 Platelet activation was measured by the detection of CD62P, CD63, and CD40L,  
290 which are localized to internal granules and expressed on platelet surface upon  
291 activation.<sup>29</sup> In the HG group, the mean fluorescence intensity (MFI) of CD62P, CD63,  
292 and CD40L on platelets activated by thrombin and collagen was significantly increased  
293 compared to the NG group (Figure 3A-C). The hyperactivation of platelets associated  
294 with diabetes were ameliorated by treating with DHM, as evidenced by inhibiting the  
295 expression of CD62P, CD63, and CD40L on platelets. Representative flow cytometry  
296 histograms are presented in Figure S2. Additionally, the expression levels of CD62P  
297 and CD63 on resting platelet isolated from mice in HG-H group were also significantly  
298 lower than those in HG group (Figure S3).

299 Integrin  $\alpha$ IIb $\beta$ 3, the most highly expressed integrin on platelets, is maintained in  
300 a low-affinity state in resting platelets. During platelet activation,  $\alpha$ IIb $\beta$ 3 changes  
301 conformation to a state capable of high-affinity ligand binding.<sup>30</sup> Therefore, we further  
302 investigated the effects of DHM on platelet  $\alpha$ IIb $\beta$ 3 activation by using JON/A, a  
303 monoclonal antibody that only binds to the activated form of integrin  $\alpha$ IIb $\beta$ 3. As  
304 shown in Figure 3D, JON/A binding induced by thrombin and collagen were  
305 significantly increased in gel-filtered platelets obtained from the HG group compared  
306 with the NG group. Treatment with DHM in HG-L and HG-H groups significantly  
307 reduced platelet  $\alpha$ IIb $\beta$ 3 activation as compared to the HG group.

### 308 **3.5 DHM reduced platelet ROS generation via potential interaction with NOX-2 and** 309 **AR active sites**



310 Considering the crucial role of ROS in platelet hyperresponsiveness associated  
311 with diabetes, we further examined the potential mechanism of DHM relative to the  
312 reduction of ROS generation in platelets. As shown in Figure 4A and B, thrombin- and  
313 collagen- stimulated ROS production in platelets were significantly enhanced in the  
314 HG group compared to the NG group ( $p < 0.001$ ). As expected, treatment with DHM  
315 inhibited platelet intracellular ROS production. Thrombin- and collagen-induced ROS  
316 generation in platelets were significantly lower in the HG-H group than in the HG group  
317 ( $p < 0.001$  and  $p < 0.01$ , respectively).

318 To explore the potential molecular mechanism by which DHM modulates platelet  
319 ROS generation, molecular docking was employed to examine whether DHM can  
320 interact with NOX-2 and AR. The results indicated that DHM could be docked into the  
321 NADPH-binding cavity of NOX-2 with a binding energy of  $-8.5$  kcal/mol. As shown in  
322 Figure 4C, DHM interacts with NOX-2 through hydrogen bonds with His119, Val228,  
323 and Arg54, a carbon hydrogen bond with His115, Pi-cation interactions with Arg54,  
324 and Pi-alkyl contacts with Ala57. These interactions, supported by extensive van der  
325 Waals contacts, suggest that DHM likely occupies a region critical for NADPH binding  
326 or electron transfer. Similarly, DHM also showed a stable binding potential within the  
327 catalytic pocket of aldose reductase (AR), with a binding energy of  $-7.7$  kcal/mol. The  
328 key stabilizing interactions include a conventional hydrogen bond with the catalytic  
329 residue His110 and a carbon hydrogen bond with Tyr48. Additional van der Waals and  
330 Pi-Alkyl contacts were observed with residues such as Trp219, Trp20, Ala299, Cys 303,  
331 Trp79, Cys298, Leu300 and Phe115 (Figure 4D). Taken together, these docking  
332 predictions suggested that DHM might interact with the amino acid residues of NOX-  
333 2 and AR active sites and thus inhibit their activities, which led to the reduction of  
334 intraplatelet ROS production.

### 335 3.6 DHM reduced plasma levels of sP-selectin and PF4 in diabetic mice

336 Plasma levels of sP-selectin and PF4 have been proposed as useful markers of *in*  
337 *vivo* platelet activation.<sup>31</sup> To further explore the effects of DHM on *in vivo* platelet  
338 activation in diabetic mice, we measured plasma levels of sP-selectin and PF4 by the



339 quantitative ELISA. As shown in Figure 5A, plasma levels of sP-selectin in diabetic mice  
340 from the HG group ( $198.97 \pm 105.54$  ng/mL) were markedly elevated compared to  
341 control mice in the NG group ( $109.63 \pm 30.49$  ng/mL,  $p < 0.001$ ). Dietary  
342 supplementation with DHM significantly attenuated the increase in both HG-L group  
343 ( $139.04 \pm 42.95$  ng/mL) and HG-H group ( $107.66 \pm 19.01$  ng/mL). Similarly, with DHM  
344 supplementation in diabetic mice, the increase of PF4 levels was dramatically  
345 attenuated but was not fully reversed to the normal level of NG group (Figure 5B).

### 346 **3.7 DHM decreased plasma TXB2 and 8-iso-PGF2 $\alpha$ in diabetic mice**

347 TXB2, the stable metabolite of thromboxane A2, which is markedly elevated in  
348 diabetes mellitus and leads to platelet hyperactivation.<sup>32</sup> In the present study, plasma  
349 levels of TXB2 were significantly higher in the HG group than in the NG group, and  
350 were normalized to the control levels after DHM treatment. As shown in Figure 5C,  
351 there were no significant differences in TXB2 levels among HG-L ( $87.24 \pm 21.78$  ng/mL),  
352 HG-H ( $82.99 \pm 16.74$  ng/mL), and NG ( $67.78 \pm 27.46$  ng/mL) groups.

353 We also detected plasma levels of 8-iso-PGF2 $\alpha$ , a stable isoprostane and reliable  
354 marker of oxidative stress *in vivo*.<sup>33</sup> As shown in Figure 5D, plasma levels of 8-iso-  
355 PGF2 $\alpha$  ( $13.83 \pm 5.16$  ng/mL) were significantly higher in the HG group than in the NG  
356 group ( $3.19 \pm 1.62$  ng/mL,  $p < 0.05$ ), and were normalized to the control levels by DHM  
357 treatment in the HG-H group ( $3.73 \pm 2.03$  ng/mL).

### 358 **3.8 DHM ameliorated thrombus formation in DM mice**

359 To investigate the effects of DHM on thrombus formation in diabetic mice, we  
360 subjected mice to collagen/epinephrine induced pulmonary embolism. In this model,  
361 collagen/epinephrine injection caused platelet activation that led to the formation of  
362 thrombi in lungs and resulted to mortality of mice. Platelet thrombi were observed in  
363 mice lung sections. Mice from the HG group showed severe pulmonary embolization,  
364 whereas DHM exerted substantial protective effects (Figure 6A). As shown in Figure  
365 6B, mice in HG group demonstrated significantly reduced length of survival relative to  
366 mice in the NG group. Intriguingly, Mice in the HG-H group exhibited significant



367 prolonged survival in contrast to the DM mice ( $p < 0.05$ ).

View Article Online  
DOI: 10.1039/D6FO00232C

368 In addition, we evaluated the effects of DHM on bleeding time via tail transection.  
369 The bleeding times of four groups were  $175.07 \pm 103.59$  s (NG group),  $145.00 \pm 48.84$   
370 s (HG group),  $149.21 \pm 70.98$  s (HG-L group), and  $178.29 \pm 82.09$  s (HG-H group). No  
371 significant differences were observed in four groups (Figure 6C). The results suggested  
372 that dietary intake of DHM reduced platelet plug formation without significantly  
373 increasing bleeding risk in diabetic mice.

### 374 **3.9 DHM potentially interacts with GPVI, PAR-1 and COX-1**

375 Molecular docking was employed to predict the binding interactions between  
376 DHM with platelet receptor PAR-1, GPVI, as well as COX-1, all of which play important  
377 roles in platelet hyperactivation in diabetes. As shown in Figure 7A, DHM showed  
378 stable binding potential within the active site of platelet GPVI. DHM formed  
379 conventional hydrogen bonds with Glu84, Ser16 and Glu138, which anchored DHM to  
380 the polar region of the pocket. Moreover, a Pi-anion interaction was observed  
381 between the aromatic ring of DHM and Glu84, further enhancing electrostatic  
382 attraction. Several surrounding residues, including Leu83, Val86, Arg142, Trp171, and  
383 Ser15, were involved in van der Waals interactions, which further reinforced the  
384 overall binding affinity. The binding energies obtained from computational docking  
385 analyses revealed that DHM exerted an even stronger binding affinity with PAR-1 ( $-9.5$   
386 kcal/mol) compared to GPVI ( $-5.9$  kcal/mol). DHM interacted with multiple  
387 surrounding amino acid residues in the binding pocket of PAR-1 through combination  
388 of hydrogen bonds and van der Waals forces. Hydrogen bonds were observed  
389 between DHM and Thr261, Glu260, Tyr337, Tyr353, and Ser344, which contributed to  
390 the initial anchoring of DHM in the pocket. Additionally, DHM formed a carbon  
391 hydrogen bond with His255. Van der Waals interactions were also prominent between  
392 DHM and various amino acids, such as Leu262, Leu332, Leu333, Ala349, Ser259,  
393 Tyr350, and His255, which collectively contributed to the binding stability (Figure 7B).  
394 These findings provide a structural basis for its inhibitory effects on platelet function  
395 activated by both collagen and thrombin.



396 Furthermore, COX-1, a key enzyme mediating TXA2 formation in platelet, was also  
397 predicted to bind stably with DHM, with a binding energy of  $-8.5$  kcal/mol. Multiple  
398 conventional hydrogen bonds were formed between DHM and Val119, Thr76, Arg79,  
399 Tyr64, and Arg83, indicating that hydrogen bonding plays a critical role in stabilizing.  
400 In addition, carbon hydrogen bonds with Gly471 contributed to ligand anchoring  
401 within the binding pocket. Extensive van der Waals interactions with His43, Gln44,  
402 Asn80 and Asn122, supplemented the overall binding stability (Figure 7C). These  
403 interactions might prevent access of arachidonic acid to the COX-1 catalytic site,  
404 leading to enzyme inactivation, which was in accordance with the reduction of plasma  
405 levels of TXB2 in DM mice. These docking results indicate potential structural bases  
406 for the inhibitory effects of DHM on platelet activation mediated by GPVI, PAR-1, and  
407 COX-1.

#### 408 4. Discussion

409 The present study demonstrated that feeding a high-fat diet in STZ-induced  
410 diabetic mice could induce *in vivo* platelet activation and platelet hyperreactivity in  
411 response to stimulation of thrombin and collagen. Dietary supplementation of DHM  
412 prevented the platelet activation, granule secretion and aggregation, decreased  
413 plasma levels of *in vivo* platelet activation markers PF4 and sP-selectin, along with  
414 oxidative and thrombogenic markers 8-iso-PGF2 $\alpha$  and TXB2. Molecular docking  
415 analysis suggested that DHM may potentially interact with key platelet surface  
416 receptors GPVI and PAR-1, as well as NOX-2, COX-1, and AR, providing a molecular  
417 basis for the observed suppression of intraplatelet ROS formation. Furthermore, DHM  
418 treatment delayed the collagen/epinephrine-induced pulmonary embolism without  
419 prolonging tail bleeding time. Given that intraplatelet ROS can act as a pivotal second  
420 messenger that enhances agonist-induced platelet activation and aggregation, we  
421 concluded that DHM could attenuate platelet hyperactivity under hyperglycemic  
422 conditions, at least in part, through the suppression of ROS generation and the  
423 downstream signaling events.

424 T2DM is a serious global metabolic health problem with high prevalence and



425 morbidity. It is now well accepted that the morbidity and mortality associated with  
426 diabetes is commonly resulted from microvascular and macrovascular  
427 complications.<sup>34</sup> Although glycemic control is the cornerstone to prevent the  
428 microvascular complications of diabetes mellitus, diabetic subjects are at a high risk of  
429 macrovascular CVD, as up to 80% of individuals with diabetes mellitus will die from  
430 cardiovascular causes.<sup>4, 35</sup> The lack of an effect of intensive glucose-lowering on most  
431 macrovascular outcomes calls for more comprehensive strategies to manage  
432 cardiovascular risk factors alongside the glycemic control.<sup>36</sup> Platelet hyperactivity,  
433 characterized by increased activation, adhesion, and aggregation of the platelets in  
434 comparison to the normal responses, has been claimed as a major contributor to the  
435 development of micro- and macro-angiopathy in patients with T2DM.<sup>37</sup> The inhibition  
436 of platelet dysfunction is an approach for preventing and treating these disorders. In  
437 the current study, platelets from diabetic mice were found to be hyper-aggregable in  
438 response to thrombin and collagen when compared to the NC mice, which is in  
439 agreement with previous observations.<sup>38</sup> DHM administration resulted in a 20%  
440 greater inhibition of platelet aggregation in diabetic mice, eliminating the hyper-  
441 aggregability in this condition and resulting in levels similar to that of the non-diabetic  
442 mice. Markers of platelet activation, such as P-selectin and CD40L, are increased in  
443 T2DM patients, which reflect a systemic prothrombotic state driven by chronic  
444 platelet hyperactivity.<sup>39</sup> In the present study, the expression of platelet surface  
445 activation antigens upon stimulation with collagen and thrombin was higher in  
446 diabetic mice than in NC mice, confirming the hyperreactivity of diabetic platelets, and  
447 it then tended to be normalized after DHM treatment.

448 Not only did platelets from DM patients show hyperresponsiveness when  
449 stimulated *in vitro*, but also they were activated *in vivo* as shown by the enhanced  
450 expression of surface activation antigens on circulating platelets, and secretion of  
451 granule contents.<sup>40</sup> In diabetic patients, elevated circulating levels of sP-selectin,  
452 sCD40L,  $\beta$ -thromboglobulin ( $\beta$ -TG), and PF4, resulting from platelet degranulation, are  
453 regarded as reliable indicators of *in vivo* platelet activation status.<sup>8, 41</sup> PF4 is a pivotal  
454 platelet-derived  $\alpha$ -granule protein released upon platelet activation, serving as a



455 critical mediator in regulating thrombotic and inflammatory responses.<sup>42</sup> Similarly, P-  
456 selectin, also stored in the platelet  $\alpha$ -granules, translocated to platelet surface during  
457 platelet activation where it is rapidly cleaved off, resulting in the release of soluble P-  
458 selectin. Plasma sP-selectin is thought to arise predominantly from activated platelets,  
459 establishing its measurement as a suitable circulating marker of *in vivo* platelet  
460 activation.<sup>31</sup> Elevated plasma sP-selectin concentrations are observed in several  
461 thrombotic diseases and are associated with the risk of developing a future vascular  
462 event.<sup>43</sup> Consistent with prior evidence, elevated plasma levels of PF4 and sP-selectin  
463 were observed in T2DM mice, confirming *in vivo* platelet activation and granule  
464 secretion in diabetic conditions.<sup>44</sup> Dietary supplementation with DHM significantly  
465 ameliorated *in vivo* platelet activation, as evidenced by reduced PF4 and sP-selectin  
466 levels, highlighting its therapeutic potential to ameliorate platelet hyperactivity and  
467 mitigate thrombotic dysregulations in diabetes.

468 Platelet hyperactivity in diabetes is a complex phenomenon that encompasses  
469 multiple mechanisms, among which oxidative stress seems to play a pivotal role.<sup>2</sup> In  
470 platelets, ROS such as superoxide anion or hydrogen peroxide, are primarily produced  
471 by NOX-2 upon stimulation with common agonists and function as second messengers  
472 to amplify platelet activation and aggregation.<sup>45</sup> DM is associated with enhanced  
473 activities of AR and NOX in platelets, resulting in overproduction of ROS, which in turn  
474 promotes lipid peroxidation and free radical-catalyzed conversion of arachidonic acid  
475 (AA) into bioactive F2-isoprostanes, such as 8-iso-prostaglandin F<sub>2</sub> $\alpha$  (8-iso-PGF<sub>2</sub> $\alpha$ ).<sup>46</sup>  
476 Elevated F2-isoprostanes production may also potentiate platelet hyperactivity by  
477 enhancing platelet response to agonist-induced platelet adhesion and aggregation, as  
478 well as by amplifying the signaling of platelet receptors.<sup>7</sup> The plasma level of 8-iso-  
479 PGF<sub>2</sub> $\alpha$  is well established to affect platelet functions and also serves as a gold-  
480 standard biomarker of oxidative stress.<sup>47</sup> In previous studies, N-acetylcysteine (NAC),  
481 a precursor of antioxidant glutathione (GSH), has been shown to attenuate platelet  
482 hyperreactivity by scavenging platelet-derived ROS in T2DM patients.<sup>48</sup> Similarly, we  
483 found that DHM supplementation in diabetic mice suppressed collagen- and  
484 thrombin-induced platelet ROS production, which was accompanied by reduced



485 plasma levels of iso-8-PGF2 $\alpha$ . Given the established role of ROS in potentiating platelet  
486 hyperactivity, the inhibitory effects of DHM on platelet hyperactivation can be  
487 explained, at least in part, by the inhibition of ROS formation. Molecular docking  
488 analysis revealed that DHM may interact with NOX-2 and AR, as well as the thrombin  
489 receptor PAR-1 and the collagen receptor GPVI, through multiple hydrogen bonds and  
490 hydrophobic interactions, which may partially explain the ROS-lowering effects of  
491 DHM observed in platelets. Moreover, DHM also exhibited favorable binding  
492 conformations with the active site of platelet COX-1, an enzyme that catalyzes AA into  
493 pro-inflammatory prostaglandins and pro-thrombotic TXA2, accompanied by  
494 production of ROS.<sup>7</sup> Although these docking simulations provide valuable mechanistic  
495 insights into how DHM may modulate platelet ROS production and function, further  
496 biochemical validation will be essential in future investigations to definitively confirm  
497 the functional blockade of these molecular targets by DHM in platelets. Furthermore,  
498 ROS are well-established as upstream regulators of classical signaling pathways that  
499 drive platelet activation, including the Syk/PLC $\gamma$ 2/calcium signaling axis, as well as  
500 PI3K/Akt, MAPKs and P53 signaling pathways.<sup>49, 50</sup> Together with previous *in vitro*  
501 study demonstrated that DHM attenuated thrombin-induced calcium mobilization  
502 and phosphorylation of ERK1/2 and p38 in platelets,<sup>20</sup> the current findings raise the  
503 possibility that under diabetic conditions, antioxidant capacity of DHM may further  
504 attenuate these downstream cascades.

505 Platelet hyperactivity in diabetes can easily lead to thrombosis and induce adverse  
506 cardiovascular event.<sup>51</sup> To determine whether dietary supplementation of DHM can  
507 reduce thrombus formation in diabetic mice, we subjected mice to a  
508 collagen/epinephrine-induced pulmonary embolism model which has been widely  
509 used to evaluate the anti-thrombotic activity of natural and dietary components.<sup>52</sup> The  
510 lung contains many small arteries and capillaries, and intravenous injection of  
511 thrombus-initiating factors such as thrombin, ADP, and collagen with epinephrine may  
512 cause fatal and acute platelet-rich thrombosis in the vasculature of lungs within a  
513 short period of time.<sup>53</sup> This *in vivo* model is largely driven by platelet activation rather  
514 than endothelial changes, which are also prominent in diabetes.<sup>27</sup> Indeed, diabetic



515 mice showed enhanced thrombus formation when compared with non-diabetic mice.  
516 DHM exhibited protective effects on pulmonary microcirculation occlusion in diabetic  
517 mice, indicated by prolonging survival time and reduced thrombotic occlusions in the  
518 lung tissue of mice in the HG-H group. Our findings are consistent with a previous  
519 study demonstrating that intravenous injection of DHM delayed FeCl<sub>3</sub>-induced carotid  
520 arterial thrombosis in mice.<sup>20</sup> Importantly, we observed that the bleeding time of  
521 DHM-treated mice in the HG-L and HG-H groups remained unchanged and were the  
522 same to the control mice, suggesting a favorable safety profile without an increased  
523 hemorrhagic risk. Additionally, previous clinical evidence has demonstrated that daily  
524 supplementation with 10 g of *Ampelopsis grossedentata* (vine tea), which provided  
525 approximately 970 mg of DHM, was both safe and effective in improving glycemic  
526 control in T2DM patients.<sup>54</sup> The dietary doses of DHM used in this study (500 and 1000  
527 mg/kg diet) correspond to an estimated human equivalent dose of approximately 300  
528 and 600 mg/day for adult, which is substantially lower than the dosage in dietary  
529 supplement interventions. Therefore, the antiplatelet effects observed in this study  
530 are physiologically achievable through the consumption of vine tea or functional food  
531 supplements. This reinforces the potential application of DHM as a safe and effective  
532 dietary strategy for preventing diabetes-related thromboembolic complication.

## 533 5. Conclusions

534 In summary, the present study demonstrated that DHM effectively ameliorated  
535 platelet dysfunction in HFD/STZ-induced diabetic mice, which may be associated with  
536 the suppression of intraplatelet ROS generation. To the best of our knowledge, this is  
537 the first study showing that dietary supplementation of DHM is able to produce  
538 beneficial platelet inhibitory effects under diabetic prothrombotic conditions.  
539 However, several limitations should be acknowledged. First, although our findings  
540 suggest a central role of ROS inhibition, the present study did not directly investigate  
541 key intracellular signaling pathways involved in platelet activation. Given the  
542 multifactorial mechanisms underlying platelet hyperreactivity in diabetes, further  
543 studies are warranted to determine whether DHM can also reverse the dysfunction of  
544 other intracellular pathways affected by diabetes mellitus in platelets. Second, the



545 P2Y12 receptor pathway plays a pivotal role in diabetic platelet hyperactivity, future  
546 studies are needed to determine whether DHM modulates ADP-induced platelet  
547 activation and aggregation, thereby providing a more comprehensive evaluation of its  
548 antiplatelet effects. Finally, further clinical studies are required to validate the efficacy  
549 of DHM supplementation and to determine the optimal doses capable of ameliorating  
550 platelet hyperreactivity in humans, which would provide a stronger basis for its clinical  
551 application. Given the growing global burden of diabetes and its associated  
552 cardiovascular complications, the identification of DHM as a promising natural  
553 candidate for managing diabetic thrombotic risk may contribute to the development  
554 of preventive nutritional strategies.

555

#### 556 **Author contributions**

557 **Fenglin Song:** Project administration, Resources, Investigation, Methodology, Writing  
558 - original draft. **Huafang Ding:** Investigation, Methodology, Writing - review. **Yun Chen:**  
559 Investigation, Methodology. **Xiangzhen Ge:** Investigation, Methodology. **Ruixue Guo:**  
560 Methodology, Writing - review. **Fangfang Wu:** Methodology, Writing - review. **Yu Guo:**  
561 Resources, Writing - review. **Ren-You Gan:** Supervision, Writing - review & editing.  
562 **Zhen-Yu Chen:** Supervision, Resources, Writing - review & editing. All authors have  
563 read and agreed to the published version of the manuscript.

#### 564 **Conflict of interest**

565 The authors declare that there is no conflict of interests.

#### 566 **Ethics statements**

567 Our study was approved by the ethics committee of Guangdong Pharmaceutical  
568 University and conformed to the Helsinki Declaration. All animal procedures were  
569 approved by the Animal Care and Protection Committee of Guangdong  
570 Pharmaceutical University (Permit No. 2023212).



571 **Data availability**

572 The original contributions presented in the study are included in the  
573 article/Supplementary Material. Further inquiries are available by contact with the  
574 corresponding author.

575 **Acknowledgements**

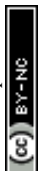
576 This work was supported by National Natural Science Foundation of China (No.  
577 81502808), The Key Projects of Social Welfare and Basic Research of Zhongshan (No.  
578 2020B2012), The Scientific Research Project of Guangdong Provincial Bureau of  
579 Traditional Chinese Medicine (No. 20252019), and Research group of functional foods  
580 development for specific populations (No. 2024ZZ12).

581

582

583 **References:**

- 584 1. Y. Zhang, Z. Wang, P. Zhou and H. Zhang, From reticulated platelets to immature platelet fraction:  
585 structure, function, and clinical applications, *Platelets*, 2025, 36, 2467383.
- 586 2. R. Kaur, M. Kaur and J. Singh, Endothelial dysfunction and platelet hyperactivity in type 2 diabetes  
587 mellitus: molecular insights and therapeutic strategies, *Cardiovasc Diabetol*, 2018, 17, 121.
- 588 3. A. K. Duttaroy, Functional Foods in Preventing Human Blood Platelet Hyperactivity-Mediated  
589 Diseases-An Updated Review, *Nutrients*, 2024, 16.
- 590 4. W. Crasto, V. Patel, M. J. Davies and K. Khunti, Prevention of Microvascular Complications of  
591 Diabetes, *Endocrinol Metab Clin North Am*, 2021, 50, 431-455.
- 592 5. A. Papazafiropoulou, N. Papanas, S. Pappas, E. Maltezos and D. P. Mikhailidis, Effects of oral  
593 hypoglycemic agents on platelet function, *J Diabetes Complications*, 2015, 29, 846-851.
- 594 6. T. Wang, J. Xu, L. Fu and L. Li, Hypertriglyceridemia is associated with platelet hyperactivation in  
595 metabolic syndrome patients, *Int J Clin Pract*, 2020, 74, e13508.
- 596 7. P. Ferroni, S. Basili, A. Falco and G. Davi, Platelet activation in type 2 diabetes mellitus, *Journal of*  
597 *thrombosis and haemostasis : JTH*, 2004, 2, 1282-1291.
- 598 8. J. H. Kim, H. Y. Bae and S. Y. Kim, Clinical marker of platelet hyperreactivity in diabetes mellitus,  
599 *Diabetes Metab J*, 2013, 37, 423-428.
- 600 9. D. Das, N. R. Shruthi, A. Banerjee, G. Jothimani, A. K. Duttaroy and S. Pathak, Endothelial dysfunction,  
601 platelet hyperactivity, hypertension, and the metabolic syndrome: molecular insights and  
602 combating strategies, *Front Nutr*, 2023, 10, 1221438.
- 603 10. A. R. Vaidya, N. Wolska, D. Vara, R. K. Mailer, K. Schroder and G. Pula, Diabetes and Thrombosis: A  
604 Central Role for Vascular Oxidative Stress, *Antioxidants (Basel)*, 2021, 10.
- 605 11. T. Geisler, N. Anders, M. Paterok, H. Langer, K. Stellos, S. Lindemann, C. Herdeg, A. E. May and M.  
606 Gawaz, Platelet response to clopidogrel is attenuated in diabetic patients undergoing coronary stent  
607 implantation, *Diabetes Care*, 2007, 30, 372-374.
- 608 12. F. Santilli, D. Lapenna, S. La Barba and G. Davi, Oxidative stress-related mechanisms affecting



- 609 response to aspirin in diabetes mellitus, *Free radical biology & medicine*, 2015, 80, 101-110. View Article Online  
DOI: 10.1039/D6FO00232C
- 610 13. D. Das, S. Adhikary, R. K. Das, A. Banerjee, A. K. Radhakrishnan, S. Paul, S. Pathak and A. K. Duttaroy,  
611 Bioactive food components and their inhibitory actions in multiple platelet pathways, *Journal of*  
612 *food biochemistry*, 2022, 46, e14476.
- 613 14. P. Y. Zhang, Cardioprotection by Phytochemicals via Antiplatelet Effects and Metabolism  
614 Modulations, *Cell Biochem Biophys*, 2015, 73, 369-379.
- 615 15. A. B. Santhakumar, M. Battino and J. M. Alvarez-Suarez, Dietary polyphenols: Structures,  
616 bioavailability and protective effects against atherosclerosis, *Food Chem Toxicol*, 2018, 113, 49-65.
- 617 16. X. Zhou, X. Huang, C. Wu, Y. Ma, W. Li, J. Hu, R. Li and F. Ya, Sulforaphane attenuates glycoprotein  
618 VI-mediated platelet mitochondrial dysfunction through up-regulating the cAMP/PKA signaling  
619 pathway in vitro and in vivo, *Food & function*, 2023, 14, 3613-3629.
- 620 17. X. Bi, X. Huang, C. Zhang, X. Zhao, J. Ma, M. Li, X. Li, B. Zeng, R. Li, X. Zhang and F. Ya, Sulforaphane  
621 attenuates aldose reductase-mediated platelet dysfunction in high glucose-stimulated human  
622 platelets via downregulation of the Src/ROS/p53 signaling pathway, *Front Nutr*, 2025, 12, 1663245.
- 623 18. L. Ye, H. Wang, S. E. Duncan, W. N. Eigel and S. F. O'Keefe, Antioxidant activities of Vine Tea  
624 (*Ampelopsis grossedentata*) extract and its major component dihydromyricetin in soybean oil and  
625 cooked ground beef, *Food Chem*, 2015, 172, 416-422.
- 626 19. H. Li, Q. Li, Z. Liu, K. Yang, Z. Chen, Q. Cheng and L. Wu, The Versatile Effects of Dihydromyricetin in  
627 Health, *Evidence-based complementary and alternative medicine: eCAM*, 2017, 2017, 1053617.
- 628 20. S. Chen, K. Lv, A. Sharda, J. Deng, W. Zeng, C. Zhang, Q. Hu, P. Jin, G. Yao, X. Xu, Z. Ming and C. Fang,  
629 Anti-thrombotic effects mediated by dihydromyricetin involve both platelet inhibition and  
630 endothelial protection, *Pharmacol Res*, 2021, 167, 105540.
- 631 21. Q. Yuan, B. Zhan, R. Chang, M. Du and X. Mao, Antidiabetic Effect of Casein Glycomacropeptide  
632 Hydrolysates on High-Fat Diet and STZ-Induced Diabetic Mice via Regulating Insulin Signaling in  
633 Skeletal Muscle and Modulating Gut Microbiota. *Nutrients*, 2020, 12, 220.
- 634 22. L. Kang, X. Ma, F. Yu, L. Xu and L. Lang, Dihydromyricetin Alleviates Non-Alcoholic Fatty Liver Disease  
635 by Modulating Gut Microbiota and Inflammatory Signaling Pathways, *J Microbiol Biotechnol*, 2024,  
636 34, 2637-2647.
- 637 23. Z. Guo, X. Chen, Z. Huang, D. Chen, B. Yu, J. He, H. Yan, P. Zheng, Y. Luo, J. Yu and H. Chen, Effect of  
638 dietary dihydromyricetin supplementation on lipid metabolism, antioxidant capacity and skeletal  
639 muscle fiber type transformation in mice, *Anim Biotechnol*, 2022, 33, 555-562.
- 640 24. F. Song, Y. Zhu, Z. Shi, J. Tian, X. Deng, J. Ren, M. C. Andrews, H. Ni, W. Ling and Y. Yang, Plant food  
641 anthocyanins inhibit platelet granule secretion in hypercholesterolaemia: Involving the signalling  
642 pathway of PI3K-Akt, *Thrombosis and haemostasis*, 2014, 112, 981-991.
- 643 25. Y. Yang, Z. Shi, A. Reheman, J. W. Jin, C. Li, Y. Wang, M. C. Andrews, P. Chen, G. Zhu, W. Ling and H.  
644 Ni, Plant food delphinidin-3-glucoside significantly inhibits platelet activation and thrombosis: novel  
645 protective roles against cardiovascular diseases, *PLoS one*, 2012, 7, e37323.
- 646 26. Y. J. Ye, L. H. Yang, M. Leng, Q. Wang, J. K. Wu, W. Wan, H. W. Wang, L. J. Li, Y. Z. Peng, S. J. Chai and  
647 Z. H. Meng, Luteolin inhibits GPVI-mediated platelet activation, oxidative stress, and thrombosis,  
648 *Frontiers in pharmacology*, 2023, 14.
- 649 27. T. P. Fidler, A. Marti, K. Gerth, E. A. Middleton, R. A. Campbell, M. T. Rondina, A. S. Weyrich and E.  
650 D. Abel, Glucose Metabolism Is Required for Platelet Hyperactivation in a Murine Model of Type 1  
651 Diabetes, *Diabetes*, 2019, 68, 932-938.
- 652 28. P. Baneu, C. Vacarescu, S. R. Dragan, L. Cirin, A. I. Lazar-Hocher, A. Cozgarca, A. A. Faur-Grigori, S.  
653 Crisan, D. Gaita, C. T. Luca and D. Cozma, The Triglyceride/HDL Ratio as a Surrogate Biomarker for  
654 Insulin Resistance, *Biomedicines*, 2024, 12.
- 655 29. A. Marginean, C. Banescu, A. Scridon and M. Dobreanu, Anti-platelet Therapy Resistance - Concept,  
656 Mechanisms and Platelet Function Tests in Intensive Care Facilities, *J Crit Care Med (Targu Mures)*,  
657 2016, 2, 6-15.
- 658 30. T. N. Durrant, M. T. van den Bosch and I. Hers, Integrin alpha(IIb)beta(3) outside-in signaling, *Blood*,  
659 2017, 130, 1607-1619.
- 660 31. P. Ferroni, F. Martini, S. Riondino, F. La Farina, A. Magnapera, F. Ciatti and F. Guadagni, Soluble P-  
661 selectin as a marker of in vivo platelet activation, *Clin Chim Acta*, 2009, 399, 88-91.
- 662 32. P. V. Halushka, R. C. Rogers, C. B. Loadholt and J. A. Colwell, Increased platelet thromboxane  
663 synthesis in diabetes mellitus, *J Lab Clin Med*, 1981, 97, 87-96.
- 664 33. C. Patrono and G. A. FitzGerald, Isoprostanes: potential markers of oxidant stress in



- 665 atherothrombotic disease, *Arteriosclerosis, thrombosis, and vascular biology*, 1997, 17, 2309-2315. View Article Online  
DOI: 10.1039/97D6FO00232C
- 666 34. J. A. Beckman, M. A. Creager and P. Libby, Diabetes and atherosclerosis: epidemiology,  
667 pathophysiology, and management, *JAMA*, 2002, 287, 2570-2581.
- 668 35. A. C. Group, A. Patel, S. MacMahon, J. Chalmers, B. Neal, L. Billot, M. Woodward, M. Marre, M.  
669 Cooper, P. Glasziou, D. Grobbee, P. Hamet, S. Harrap, S. Heller, L. Liu, G. Mancia, C. E. Mogensen, C.  
670 Pan, N. Poulter, A. Rodgers, B. Williams, S. Bompaint, B. E. de Galan, R. Joshi and F. Travert, Intensive  
671 blood glucose control and vascular outcomes in patients with type 2 diabetes, *N Engl J Med*, 2008,  
672 358, 2560-2572.
- 673 36. S. K. Kunutsor, V. G. Balasubramanian, F. Zaccardi, C. L. Gillies, V. R. Aroda, S. Seidu and K. Khunti,  
674 Glycaemic control and macrovascular and microvascular outcomes: A systematic review and meta-  
675 analysis of trials investigating intensive glucose-lowering strategies in people with type 2 diabetes,  
676 *Diabetes Obes Metab*, 2024, 26, 2069-2081.
- 677 37. A. Gaiz, S. Mosawy, N. Colson and I. Singh, Thrombotic and cardiovascular risks in type two diabetes;  
678 Role of platelet hyperactivity, *Biomedicine & pharmacotherapy*, 2017, 94, 679-686.
- 679 38. M. Henry, L. Davidson, Z. Cohen, P. F. McDonagh, P. E. Nolan and L. S. Ritter, Whole blood  
680 aggregation, coagulation, and markers of platelet activation in diet-induced diabetic C57BL/6J mice,  
681 *Diabetes Res Clin Pract*, 2009, 84, 11-18.
- 682 39. A. I. Vinik, T. Erbas, T. S. Park, R. Nolan and G. L. Pittenger, Platelet dysfunction in type 2 diabetes,  
683 *Diabetes Care*, 2001, 24, 1476-1485.
- 684 40. F. Rollini, F. Franchi, A. Muniz-Lozano and D. J. Angiolillo, Platelet function profiles in patients with  
685 diabetes mellitus, *J Cardiovasc Transl Res*, 2013, 6, 329-345.
- 686 41. P. Kubisz, L. Stanciakova, J. Stasko, P. Galajda and M. Moka, Endothelial and platelet markers in  
687 diabetes mellitus type 2, *World J Diabetes*, 2015, 6, 423-431.
- 688 42. M. A. Kowalska, L. Rauova and M. Poncz, Role of the platelet chemokine platelet factor 4 (PF4) in  
689 hemostasis and thrombosis, *Thrombosis research*, 2010, 125, 292-296.
- 690 43. P. M. Ridker, J. E. Buring and N. Rifai, Soluble P-selectin and the risk of future cardiovascular events,  
691 *Circulation*, 2001, 103, 491-495.
- 692 44. S. J. Israels, A. McNicol, H. J. Dean, F. Cognasse and E. A. Sellers, Markers of platelet activation are  
693 increased in adolescents with type 2 diabetes, *Diabetes Care*, 2014, 37, 2400-2403.
- 694 45. B. Wachowicz, B. Olas, H. M. Zbikowska and A. Buczynski, Generation of reactive oxygen species in  
695 blood platelets, *Platelets*, 2002, 13, 175-182.
- 696 46. N. Vazzana, P. Ranalli, C. Cuccurullo and G. Davi, Diabetes mellitus and thrombosis, *Thrombosis  
697 research*, 2012, 129, 371-377.
- 698 47. A. Mezzetti, F. Cipollone and F. Cuccurullo, Oxidative stress and cardiovascular complications in  
699 diabetes: isoprostanes as new markers on an old paradigm, *Cardiovasc Res*, 2000, 47, 475-488.
- 700 48. K. R. Gibson, T. J. Winterburn, F. Barrett, S. Sharma, S. M. MacRury and I. L. Megson, Therapeutic  
701 potential of N-acetylcysteine as an antiplatelet agent in patients with type-2 diabetes, *Cardiovasc  
702 Diabetol*, 2011, 10, 43.
- 703 49. W. H. Tang, J. Stitham, Y. Jin, R. Liu, S. H. Lee, J. Du, G. Atteya, S. Gleim, G. Spollett, K. Martin and J.  
704 Hwa, Aldose reductase-mediated phosphorylation of p53 leads to mitochondrial dysfunction and  
705 damage in diabetic platelets, *Circulation*, 2014, 129, 1598-1609.
- 706 50. M. K. Delaney, K. Kim, B. Estevez, Z. Xu, A. Stojanovic-Terpo, B. Shen, M. Ushio-Fukai, J. Cho and X.  
707 Du, Differential Roles of the NADPH-Oxidase 1 and 2 in Platelet Activation and Thrombosis,  
708 *Arteriosclerosis, thrombosis, and vascular biology*, 2016, 36, 846-854.
- 709 51. S. Ebara, M. Marumo, J. Mukai, M. Ohki, K. Uchida and I. Wakabayashi, Relationships of oxidized  
710 HDL with blood coagulation and fibrinolysis in patients with type 2 diabetes mellitus, *J Thromb  
711 Thrombolysis*, 2018, 45, 200-205.
- 712 52. L. Kim, Y. Lim, S. Y. Park, Y. J. Kim, O. Kwon, J. H. Lee, J. H. Shin, Y. K. Yang and J. Y. Kim, A comparative  
713 study of the antithrombotic effect through activated endothelium of garlic powder and tomato  
714 extracts using a rodent model of collagen and epinephrine induced thrombosis, *Food Sci Biotechnol*,  
715 2018, 27, 1513-1518.
- 716 53. R. Miao, J. Liu and J. Wang, Overview of mouse pulmonary embolism models, *Drug Discovery Today:  
717 Disease Models*, 2010, 7, 77-82.
- 718 54. L. Ran, X. Wang, H. Lang, J. Xu, J. Wang, H. Liu, M. Mi and Y. Qin, Ampelopsis grossedentata  
719 supplementation effectively ameliorates the glycemic control in patients with type 2 diabetes  
720 mellitus, *Eur J Clin Nutr*, 2019, 73, 776-782.



721

722

723

[View Article Online](#)  
DOI: 10.1039/D6FO00232C

Food & Function Accepted Manuscript



724

View Article Online  
DOI: 10.1039/D6FO00232C**Table 1 Effects of DHM administration on the body weight, average food intake, and organ index in T2DM mice.**

Groups	NG	HG	HG-L	HG-H
Initial Body weight (g)	20.70 ± 1.41	20.99 ± 1.21	20.21 ± 1.23	20.52 ± 1.18
Final Body weight (g)	29.37 ± 2.43 <sup>a</sup>	32.80 ± 3.58 <sup>b</sup>	32.61 ± 2.76 <sup>b</sup>	30.36 ± 2.56 <sup>a</sup>
Food intake (g/d)	3.64 ± 0.19	3.27 ± 0.28	3.10 ± 0.27	3.21 ± 0.23
Organ index (%)				
Heart	0.57 ± 0.11	0.56 ± 0.07	0.51 ± 0.09	0.56 ± 0.07
Liver	4.43 ± 0.42 <sup>a</sup>	5.21 ± 0.73 <sup>b</sup>	4.93 ± 0.50 <sup>b</sup>	4.88 ± 0.50 <sup>b</sup>
Spleen	0.33 ± 0.07	0.35 ± 0.08	0.31 ± 0.09	0.31 ± 0.08
Pulmonary	0.69 ± 0.18	0.66 ± 0.12	0.68 ± 0.06	0.69 ± 0.12
Kidney	1.32 ± 0.13 <sup>a</sup>	1.31 ± 0.11 <sup>a</sup>	1.29 ± 0.11 <sup>b</sup>	1.33 ± 0.13 <sup>a</sup>

725 NG, normal control mice; HG, high glycemia model group; HG-L, high glycemia group with a low  
 726 dose of dihydromyricetin (DHM) (500 mg/kg); HG-H, high glycemia group with a high dose of DHM  
 727 (1000 mg/kg). The organ index was calculated as the organ-to-body weight ratio (relative weight,  
 728 percentage). Data are presented as the mean ± SD (n = 20). Different lowercase letters within the  
 729 same row indicate significant differences between groups ( $p < 0.05$ ).

730

731

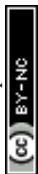
732

**Table 2 Effects of DHM supplementation on fasting blood glucose and plasma lipid profile in T2DM mice.**

734

Groups	NG	HG	HG-L	HG-H
FBG (mmol/L)	8.56 ± 1.01 <sup>a</sup>	21.15 ± 3.67 <sup>b</sup>	18.01 ± 7.35 <sup>b</sup>	16.51 ± 3.76 <sup>c</sup>
TC (mmol/L)	1.75 ± 0.21 <sup>a</sup>	1.60 ± 0.20 <sup>ab</sup>	1.60 ± 0.19 <sup>ab</sup>	1.58 ± 0.22 <sup>b</sup>
TG (mmol/L)	1.08 ± 0.24 <sup>a</sup>	1.35 ± 0.33 <sup>a</sup>	1.38 ± 0.40 <sup>b</sup>	1.11 ± 0.35 <sup>a</sup>
HDL (mmol/L)	1.14 ± 0.16 <sup>a</sup>	0.97 ± 0.10 <sup>b</sup>	1.00 ± 0.10 <sup>b</sup>	0.97 ± 0.12 <sup>b</sup>
LDL (mmol/L)	0.53 ± 0.19	0.55 ± 0.16	0.53 ± 0.12	0.53 ± 0.16
TG/HDL-C	0.95 ± 0.19 <sup>a</sup>	1.40 ± 0.35 <sup>b</sup>	1.41 ± 0.48 <sup>b</sup>	1.13 ± 0.36 <sup>a</sup>

735 NG, normal control mice; HG, high glycemia model group; HG-L, high glycemia group with a low  
 736 dose of dihydromyricetin (DHM) (500 mg/kg); HG-H, high glycemia group with a high dose of DHM  
 737 (1000 mg/kg). Data are presented as the mean ± SD (n = 14). Different lowercase letters within the



738 same row indicate significant differences between groups ( $p < 0.05$ ).

739

740

View Article Online  
DOI: 10.1039/D6FO00232C



741 **Figure Legends**

742

743 **Figure 1. Effects of DHM administration on diabetic platelet aggregation.**

744 Gel-filtered platelets were prepared from the normal control and T2DM mice. Platelet  
745 aggregation responses were induced by 0.1 U/mL thrombin (A) or 1 µg/mL collagen  
746 (B) in an aggregometer. Aggregation was turbidimetrically assessed and expressed as  
747 percent change in light transmission. NG, normal control mice; HG, high glycemia  
748 model group; HG-L, high glycemia group with a low dose of dihydromyricetin (DHM)  
749 (500 mg/kg); HG-H, high glycemia group with a high dose of DHM (1000 mg/kg). Data  
750 are presented as the mean ± SD (n = 7 independent biological replicates, each pooled  
751 from two mice per group). \*  $p < 0.05$ , \*\*  $p < 0.01$ , and \*\*\*  $p < 0.001$ .

752

753 **Figure 2. Effects of DHM supplementation on diabetic platelet ATP secretion.**

754 Gel-filtered platelets from normal control and T2DM mice were incubated with  
755 luciferin-luciferase reagent before being stimulated with 0.1 U/mL thrombin. (A) or 1  
756 µg/mL collagen (B). ATP secretion from platelet dense granules was determined in a  
757 Chrono-log lumi-aggregometer and expressed as nmol/mL. NG, normal control mice;  
758 HG, high glycemia model group; HG-L, high glycemia group with a low dose of  
759 dihydromyricetin (DHM) (500 mg/kg); HG-H, high glycemia group with a high dose of  
760 DHM (1000 mg/kg). Data are presented as the mean ± SD (n = 7 independent biological  
761 replicates, each pooled from two mice per group). \*  $p < 0.05$ , \*\*  $p < 0.01$ , and \*\*\*  $p < 0.001$ .

762

763  
764 **Figure 3. Effects of DHM on diabetic platelet surface expression of P-selectin, CD63,  
765 CD40L, and activated integrin αIIbβ3.**

766 Platelet activation markers were analyzed by flow cytometry after stimulation by  
767 thrombin (0.1 U/mL) or collagen (1 µg/mL). (A) P-selectin expression on platelet in  
768 response to thrombin or collagen, (B) surface expression of CD63, (C) surface  
769 expression of CD40L, (D) binding of PE-labeled JON/A antibody to platelets, which  
770 represents integrin αIIbβ3 activation. NG, normal control mice; HG, high glycemia  
771 model group; HG-L, high glycemia group with a low dose of dihydromyricetin (DHM)  
772 (500 mg/kg); HG-H, high glycemia group with a high dose of DHM (1000 mg/kg). Data  
773 are presented as the mean ± SD (n = 7 independent biological replicates, each pooled  
774 from two mice per group). \*  $p < 0.05$ , \*\*  $p < 0.01$ , and \*\*\*  $p < 0.001$ .

775

776 **Figure 4. Effects of DHM on intraplatelet ROS formation and molecular docking  
777 analysis with NOX-1 and AR.**

778 Generation of ROS was quantified by flow cytometry using 5-(and 6)-chloromethyl-  
779 2',7'-dichlorodihydrofluorescein diacetate (CM-H2DCFDA). Gel-filtered platelets  
780 separated from mice were loaded with CM-H2DCFDA dye and stimulated with (A) 0.5  
781 U/mL thrombin or (B) 2 µg/mL collagen. (C) Molecular interaction diagram of DHM  
782 with NOX-2. (D) Molecular interaction diagram of DHM with AR. NG, normal control  
783 mice; HG, high glycemia model group; HG-L, high glycemia group with a low dose of  
784 dihydromyricetin (DHM) (500 mg/kg); HG-H, high glycemia group with a high dose of



785 DHM (1000 mg/kg). Data are presented as the mean  $\pm$  SD (n = 7). \*  $p < 0.05$ , \*\*  $p < 0.01$ , and \*\*\*  $p < 0.001$ . [View Article Online](#)  
786 [DOI: 10.1039/D6FO00232C](#)

787

788 **Figure 5. Effects of DHM on plasma levels of sP-selectin, PF4, TXB2, and 8-iso-PGF2 $\alpha$**   
789 **in T2DM mice.**

790 The plasma levels of sP-selectin (A), PF4 (B), TXB2 (C), and 8-iso-PGF2 $\alpha$  (D) were  
791 measured by ELISA. NG, normal control mice; HG, high glycemia model group; HG-L,  
792 high glycemia group with a low dose of dihydromyricetin (DHM) (500 mg/kg); HG-H,  
793 high glycemia group with a high dose of DHM (1000 mg/kg). Data are presented as the  
794 mean  $\pm$  SD (n = 14). \*  $p < 0.05$ , \*\*  $p < 0.01$ , and \*\*\*  $p < 0.001$ .

795

796 **Figure 6. Effects of DHM consumption on acute pulmonary thrombus formation in**  
797 **T2DM mice.**

798 T2DM mice were fed with high fat diet supplemented with DHM for 8 weeks. Acute  
799 pulmonary thromboembolism was then initiated by collagen/epinephrine injection,  
800 and the surviving time of mice were recorded. (A) Representative hematoxylin and  
801 eosin-stained images of lung sections. (B) Survival curves of mice subjected to  
802 collagen/epinephrine-induced pulmonary embolism (n = 6 per group). ###  $p < 0.001$   
803 compared to the NG group. \*\*  $p < 0.01$  compared to the HG group, Log-rank (Mantel-  
804 Cox) test. (C) Tail bleeding time measured after amputating 2 mm of the tail tip (n =  
805 14). NG, normal control mice; HG, high glycemia model group; HG-L, high glycemia  
806 group with a low dose of dihydromyricetin (DHM) (500 mg/kg); HG-H, high glycemia  
807 group with a high dose of DHM (1000 mg/kg). Data are presented as the mean  $\pm$  SD.  
808 No significant differences in bleeding times were observed among four groups.

809

810 **Figure 7. Molecular docking analysis of DHM with GPVI, PAR-1 and COX-1.**

811 Molecular docking analysis showing the 3D and 2D interaction diagrams of DHM with  
812 GPVI (A), PAR-1(B) and COX-1 (C).

813

814



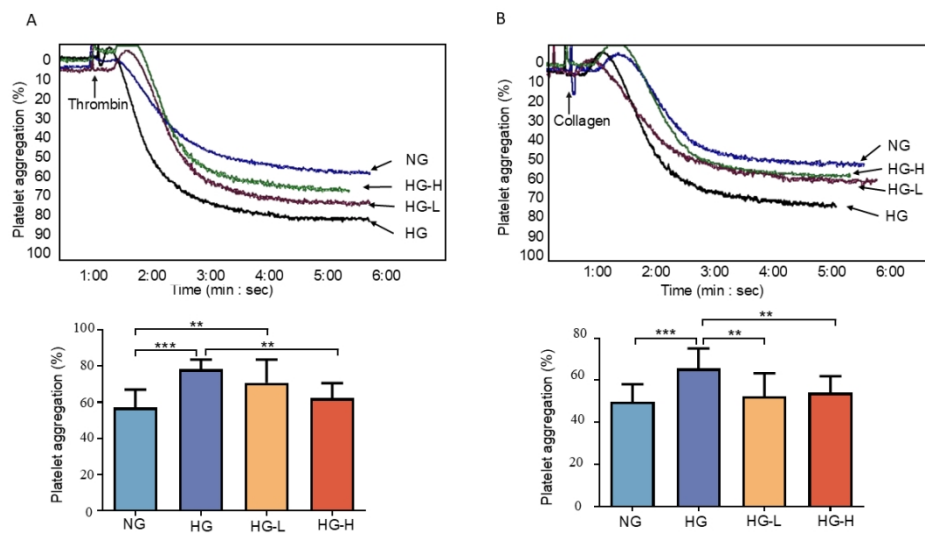


Figure 1. Effects of DHM administration on diabetic platelet aggregation. Gel-filtered platelets were prepared from the normal control and T2DM mice. Platelet aggregation responses were induced by 0.1 U/mL thrombin (A) or 1  $\mu$ g/mL collagen (B) in an aggregometer. Aggregation was turbidimetrically assessed and expressed as percent change in light transmission. NG, normal control mice; HG, high glycemia model group; HG-L, high glycemia group with a low dose of dihydromyricetin (DHM) (500 mg/kg); HG-H, high glycemia group with a high dose of DHM (1000 mg/kg). Data are presented as the mean  $\pm$  SD ( $n = 7$  independent biological replicates, each pooled from two mice per group). \*  $p < 0.05$ , \*\*  $p < 0.01$ , and \*\*\*  $p < 0.001$ .

338x190mm (96 x 96 DPI)



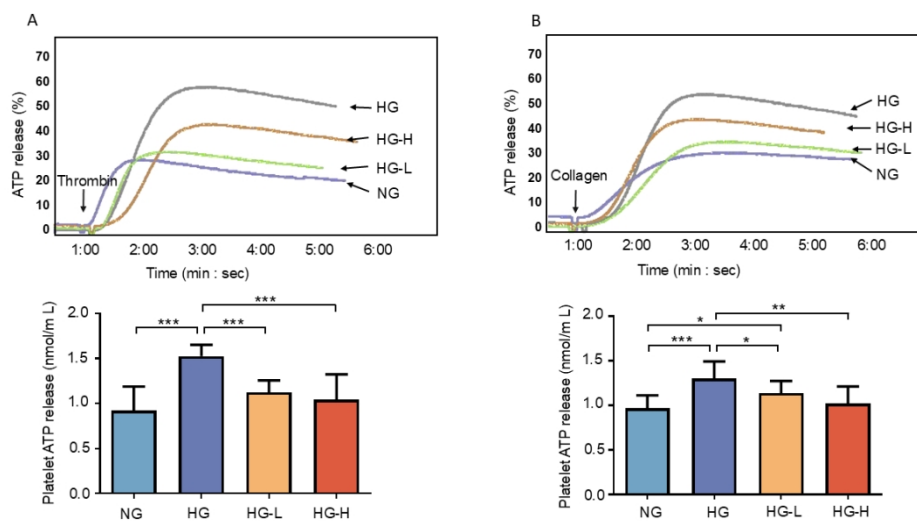


Figure 2. Effects of DHM supplementation on diabetic platelet ATP secretion.

Gel-filtered platelets from normal control and T2DM mice were incubated with luciferin-luciferase reagent before being stimulated with 0.1 U/mL thrombin. (A) or 1  $\mu$ g/mL collagen (B). ATP secretion from platelet dense granules was determined in a Chrono-log lumi-aggregometer and expressed as nmol/mL. NG, normal control mice; HG, high glycemia model group; HG-L, high glycemia group with a low dose of dihydromyricetin (DHM) (500 mg/kg); HG-H, high glycemia group with a high dose of DHM (1000 mg/kg). Data are presented as the mean  $\pm$  SD ( $n = 7$  independent biological replicates, each pooled from two mice per group). \*  $p < 0.05$ , \*\*  $p < 0.01$ , and \*\*\*  $p < 0.001$ .

338x190mm (96 x 96 DPI)



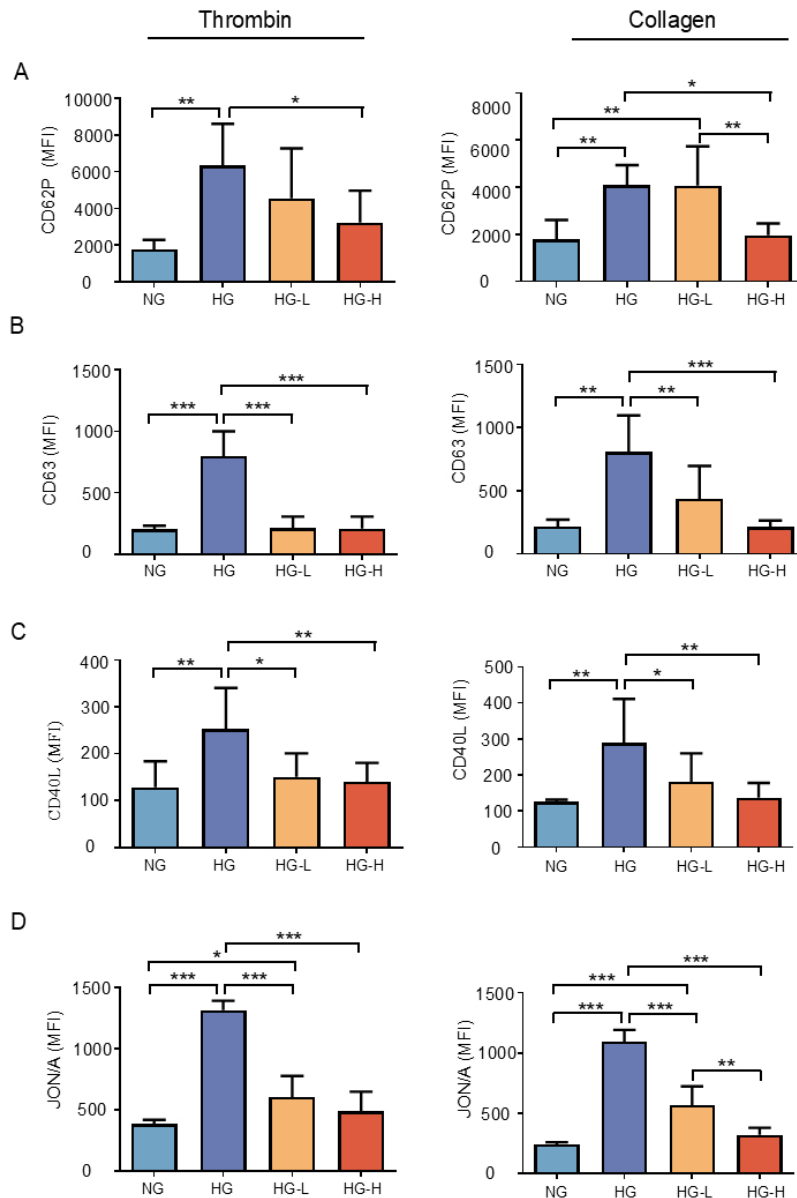


Figure 3. Effects of DHM on diabetic platelet surface expression of P-selectin, CD63, CD40L, and activated integrin  $\alpha$ IIb $\beta$ 3.

Platelet activation markers were analyzed by flow cytometry after stimulation by thrombin (0.1 U/mL) or collagen (1  $\mu$ g/mL). (A) P-selectin expression on platelet in response to thrombin or collagen, (B) surface expression of CD63, (C) surface expression of CD40L, (D) binding of PE-labeled JON/A antibody to platelets, which represents integrin  $\alpha$ IIb $\beta$ 3 activation. NG, normal control mice; HG, high glycemia model group; HG-L, high glycemia group with a low dose of dihydromyricetin (DHM) (500 mg/kg); HG-H, high glycemia group with a high dose of DHM (1000 mg/kg). Data are presented as the mean  $\pm$  SD ( $n = 7$  independent biological replicates, each pooled from two mice per group). \*  $p < 0.05$ , \*\*  $p < 0.01$ , and \*\*\*  $p < 0.001$ .

190x275mm (96 x 96 DPI)



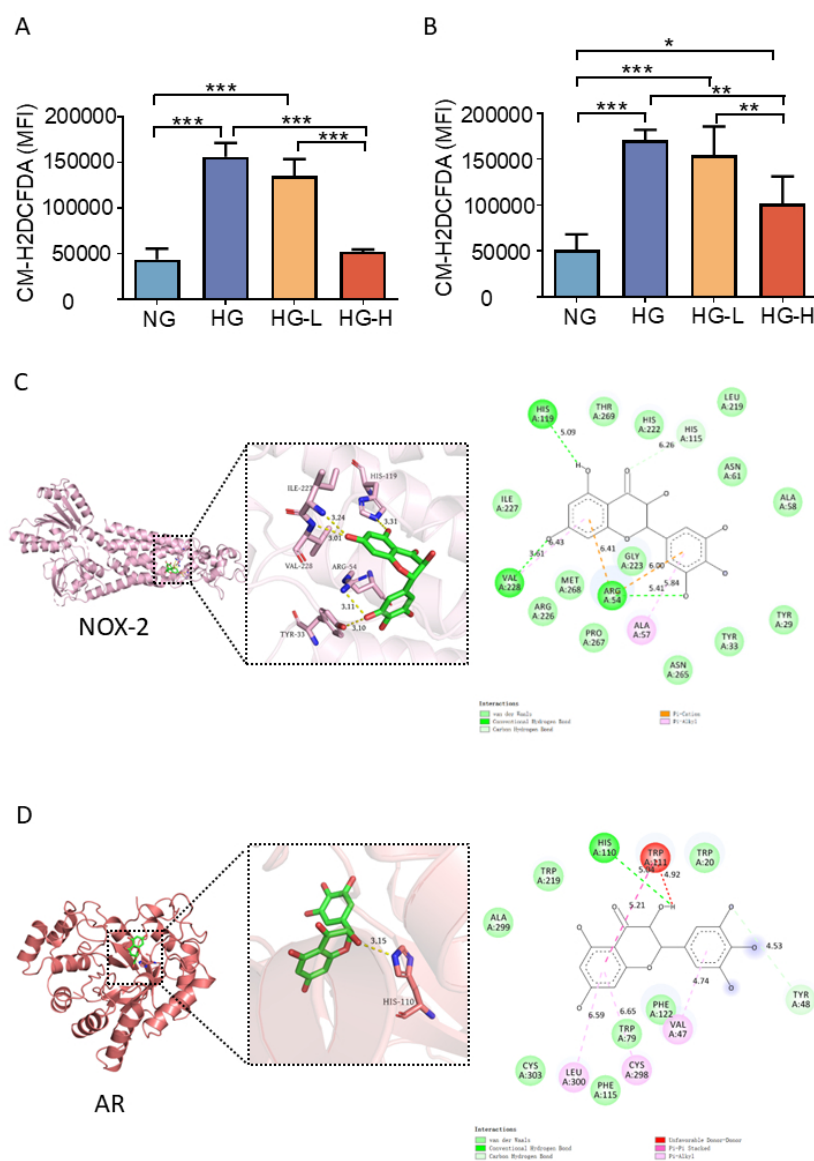


Figure 4. Effects of DHM on intraplatelet ROS formation and molecular docking analysis with NOX-1 and AR.

Generation of ROS was quantified by flow cytometry using 5-(and 6)-chloromethyl-2',7'-dichlorodihydrofluorescein diacetate (CM-H2DCFDA). Gel-filtered platelets separated from mice were loaded with CM-H2DCFDA dye and stimulated with (A) 0.5 U/mL thrombin or (B) 2  $\mu$ g/mL collagen. (C) Molecular interaction diagram of DHM with NOX-2. (D) Molecular interaction diagram of DHM with AR. NG, normal control mice; HG, high glycemia model group; HG-L, high glycemia group with a low dose of dihydromyricetin (DHM) (500 mg/kg); HG-H, high glycemia group with a high dose of DHM (1000 mg/kg). Data are presented as the mean  $\pm$  SD ( $n = 7$ ). \*  $p < 0.05$ , \*\*  $p < 0.01$ , and \*\*\*  $p < 0.001$ .

190x275mm (96 x 96 DPI)



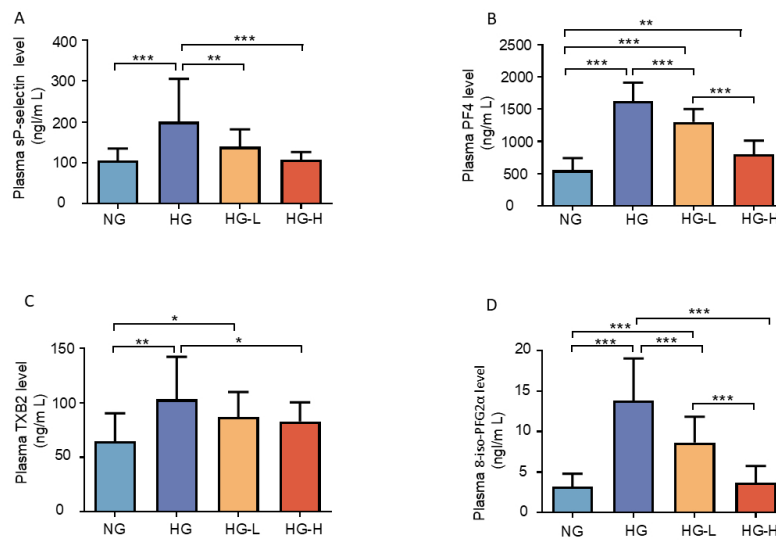


Figure 5. Effects of DHM on plasma levels of sP-selectin, PF4, TXB2, and 8-iso-PGF2a in T2DM mice. The plasma levels of sP-selectin (A), PF4 (B), TXB2 (C), and 8-iso-PGF2a (D) were measured by ELISA. NG, normal control mice; HG, high glycemia model group; HG-L, high glycemia group with a low dose of dihydromyricetin (DHM) (500 mg/kg); HG-H, high glycemia group with a high dose of DHM (1000 mg/kg). Data are presented as the mean  $\pm$  SD ( $n = 14$ ). \*  $p < 0.05$ , \*\*  $p < 0.01$ , and \*\*\*  $p < 0.001$ .

338x190mm (96 x 96 DPI)



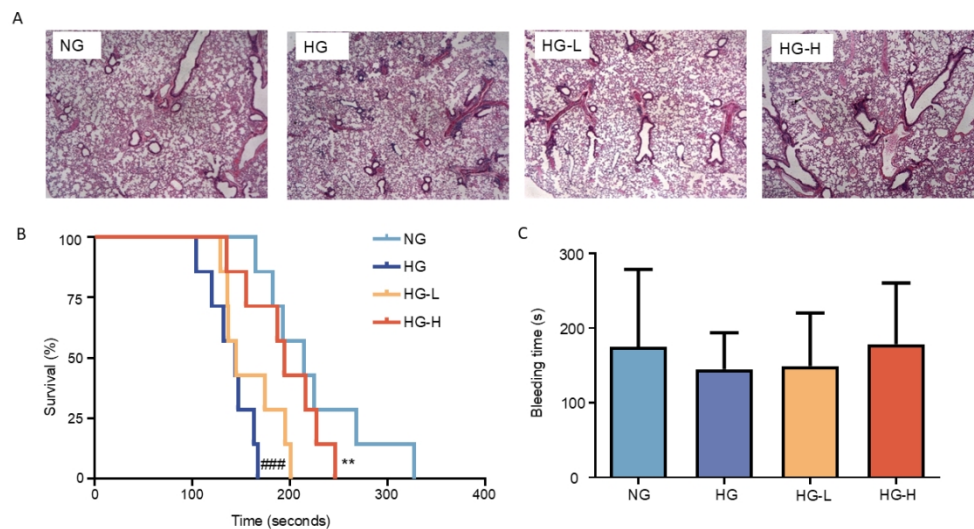


Figure 6. Effects of DHM consumption on acute pulmonary thrombus formation in T2DM mice.

T2DM mice were fed with high fat diet supplemented with DHM for 8 weeks. Acute pulmonary thromboembolism was then initiated by collagen/epinephrine injection, and the surviving time of mice were recorded. (A) Representative hematoxylin and eosin-stained images of lung sections. (B) Survival curves of mice subjected to collagen/epinephrine-induced pulmonary embolism ( $n = 6$  per group). ###  $p < 0.001$  compared to the NG group. \*\*  $p < 0.01$  compared to the HG group, Log-rank (Mantel-Cox) test. (C) Tail bleeding time measured after amputating 2 mm of the tail tip ( $n = 14$ ). NG, normal control mice; HG, high glycemia model group; HG-L, high glycemia group with a low dose of dihydromyricetin (DHM) (500 mg/kg); HG-H, high glycemia group with a high dose of DHM (1000 mg/kg). Data are presented as the mean  $\pm$  SD. No significant differences in bleeding times were observed among four groups.

338x190mm (96 x 96 DPI)



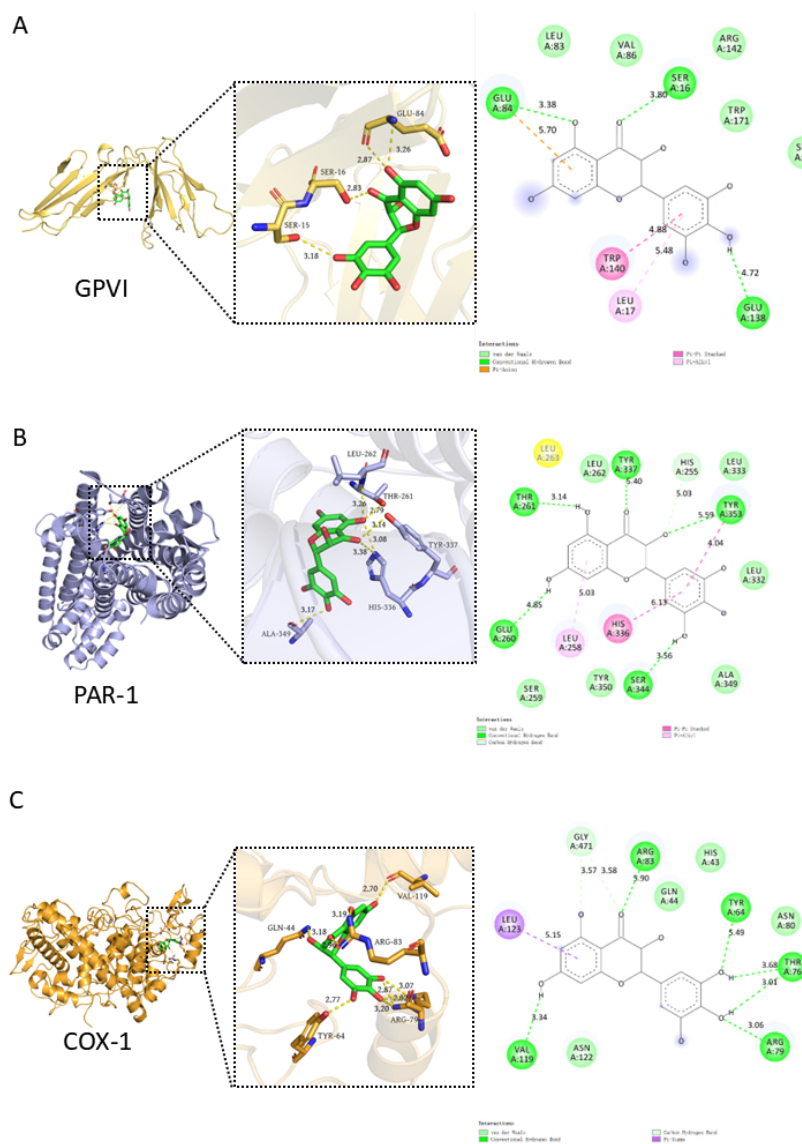


Figure 7. Molecular docking analysis of DHM with GPVI, PAR-1 and COX-1. Molecular docking analysis showing the 3D and 2D interaction diagrams of DHM with GPVI (A), PAR-1(B) and COX-1 (C).

190x275mm (96 x 96 DPI)



View Article Online  
DOI: 10.1039/D6FO00232C

## Data availability Statement

The original contributions presented in the study are included in the article/Supplementary Material. Further inquiries are available by contact with the corresponding author.

